

PPA: Preference Profiling Attack Against Federated Learning

Chunyi Zhou

zhouchunyi@njust.edu.cn

Nanjing University of Science and Technology.

Kai Chen

chenkai@iie.ac.cn

Chinese Academy of Science.

Yansong Gao

yansong.gao@njust.edu.cn

Nanjing University of Science and Technology.

Anmin Fu

fuam@njust.edu.cn

Nanjing University of Science and Technology.

Minhui Xue

jason.xue@adelaide.edu.au

The University of Adelaide, Australia.

Zhiyang Dai

dzy@njust.edu.cn

Nanjing University of Science and Technology.

Zhi Zhang

zhi.zhang@data61.csiro.au

Data61, CSIRO, Australia.

Yuqing Zhang

zhangyq@ucas.ac.cn

University of Chinese Academy of Science.

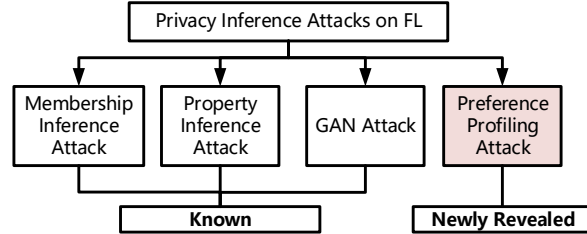


Figure 1: Privacy inference attacks on FL. Orthogonal to known attacks on the left, we reveal a new type of inference attack on the right, i.e., preference profiling attack.

KEYWORDS

Federated Learning, Privacy Inference Attack, Preference Profiling Attack

1 INTRODUCTION

As traditional centralized deep learning requires centralizing user data, it can be abused to leak user data privacy and breaches the national regulations such as the General Data Protection Regulation (GDPR) [35], California Privacy Rights Act (CPRA) [42], and China Data Security Law (CDSL) [10]. In contrast to centralized learning, Federated learning (FL) [29] voids the requirement by using local user model updates rather than raw user data, significantly mitigating data privacy issues [4, 49, 52, 59]. As such, FL has become the most popular distributed machine learning technique and empowered a wide range of privacy-sensitive applications, e.g., smart healthcare, social network, and wireless communication [9, 33, 40, 43, 56, 58].

State of the arts and limitations: Nonetheless, private user information in FL can still be leaked by inference attacks [7, 27, 31], as summarized in Figure 1. To date, there are three known privacy inference attacks. Specifically, membership inference [32, 39] determines whether a particular data record is used for training a victim user's uploaded model. Property inference [13, 30] determines whether a target attribute exists in a victim user's local dataset. Generative Adversarial Networks (GAN) [18, 47] reverse

ABSTRACT

Federated learning (FL) trains a global model across a number of decentralized participants, each with a local dataset. Compared to traditional centralized learning, FL does not require direct local datasets access and thus mitigates data security and privacy concerns. However, data privacy concerns for FL still exist due to inference attacks, including known membership inference, property inference, and data inversion.

In this work, we reveal a new type of privacy inference attack, coined Preference Profiling Attack (PPA), that accurately profiles private preferences of a local user, e.g., most liked/disliked items of online shopping and selfie expressions of photos. In general, the PPA can profile top- k (e.g., $k = 1, 2, 3$), especially for top-1, preferences contingent on the local user's characteristics. Our key insight is that the gradient variation of a local user's model has a distinguishable sensitivity to the sample proportion of a given class, especially the majority/minority class. By observing a user model's gradient sensitivity to a class, the PPA can profile the sample proportion of the class in the user's local dataset and thus *the user's preference of the class* is exposed. The inherent statistical heterogeneity of FL further facilitates the PPA. We have extensively evaluated the PPA's effectiveness using four datasets from the image domains of MNIST, CIFAR10, Products-10K and RAF-DB. Our results show that the PPA achieves 90% and 98% top-1 attack accuracy to the MNIST and CIFAR10, respectively. More importantly, in the real-world commercial scenarios of shopping (i.e., Products-10K) and the social network (i.e., RAF-DB), the PPA gains a top-1 attack accuracy of 78% in the former case to infer the most ordered items (e.g., as a commercial competitor), and 88% in the latter case to infer a victim user's emotions, e.g., disgusted from her selfies. The top-3 attack accuracy of RAF-DB and top-2 accuracy is up to 88% and 100% for the Products-10K and RAF-DB, respectively. We also show that the PPA is insensitive to the number of FL's local users (up to 100 we tested) and local training epochs (up to 20 we tested) used by a user. Although existing countermeasures such as dropout and differential privacy protection can lower the PPA's accuracy to some extent, they unavoidably incur notable global model deterioration.

engineers images of a target label based on the model uploaded by a victim user. Inference attacks pose severe threats to user privacy in FL [28]. In privacy-sensitive applications, an attacker can exploit them to leak their interested victim’s private information. For example, in a DNA determination task, the membership inference attack can utilize a statistical distance measure to determine if a known individual is in a mixture of DNA [15].

None of the aforementioned privacy inference attacks can profile FL user data preference, which is one of the most interesting private information an attacker would like to infer, akin to profiling users in social networks [2, 5, 50]. For instance, in an FL-based recommendation system [1, 37, 51], an attacker would be interested in items liked/disliked by a user who is a participant in FL. The most/least on-sale groceries of a shopping mall is also an appealing target for a commercial competitor. In this context, we ask the following questions:

Is it feasible to profile user data preference in FL? If so, how can we make the preference profiling attack as effective as possible?

PPA: We provide an affirmative answer, in which we demonstrate that effectively profiling user preference can be practically achieved by leveraging our presented techniques. A pragmatic PPA is mainly built upon our key observation.

Key Observation: A model memorizes the data-distribution characteristic of a training dataset, and inadvertently reflects it in the form of gradient changes, that is, when the model is being trained upon a dataset, its gradient change is related to the sample size of a class. For example, if data that does not exist or has a small amount in the dataset, the model does not have the ability of generalization at the beginning. Thus, the model will exhibit *a greater gradient effect to change the weights of the corresponding neurons to minimize the expected loss of the model*. That is, the gradient change or sensitivity in the model training process is inversely proportional to the sample size of a class: a large (small) gradient change or sensitivity will be introduced when the sample size of a class is small (large) (detailed in Section 5.1). Additionally, the FL is with two inherent characteristics: system and statistical heterogeneity [20, 25]. The statistical heterogeneity means that FL users have different data distribution in reality, and amplifies the gradient sensitivity discrepancies among diverse classes of the local dataset, which facilitates the PPA.

Challenges: To achieve PPA, there are three main challenges in making PPA effective.

- How to extract and quantify the gradient sensitivity of a local model per class/label?
- How to improve the precision of the gradient sensitivity in a fine-grained manner?
- How to profile the sample size proportion of a class label given the quantified sensitivity?

Our Solutions: For the first challenge, given a user uploaded model, we iteratively retrain it with a few samples per class to extract the gradient sensitivity/variations. A larger sample size proportion of class leads to a lower sensitivity. For the second challenge, we strategically select a subset of users, disguised within a common sampling strategy used in FL, to aggregate a subset of models of interested users for the global model update. We call it selective aggregation. Because trivially aggregating all models

will conceal per user’s data characteristics, rendering difficulty of saliently extracting the local model sensitivity in the consecutive rounds. This allows the attacker to gain fine-grained sensitive information of interested users in the next FL round while not degrading the global model utility, thus still remaining stealthy. As for the last challenge, we leverage an attack model that is a meta-classifier to automatically predict targeted user data preference by feeding the extracted sensitivity information of user uploaded model and aggregated model as inputs.

Contributions: We have made three main contributions:

- We reveal a new type of privacy inference attack, Preference Profiling Attack (PPA), on FL. By exploiting the fact that the model memorizes the data preference (i.e., Majority/Minority class) and leaves traces, we construct a model sensitivity extraction algorithm to determine the gradient change of each class. Through the designed meta-classifier, PPA can infer the preference class of the user’s dataset in FL.
- We design a selective aggregation mechanism to greatly improve the success rate of PPA and alleviate the cancellation effect of intuitive global model aggregation on inference attacks. It aggregates a victim user’s model with k models with the highest (lowest) model sensitivity of majority (minority) class, that is, the model sensitivity of k local models to the victim local model’s majority (minority) class is opposed to that of the targeted local model. The operation can amplify the *differential model sensitivity*, significantly improving efficacy of the meta-classifier for better attack accuracy.
- We perform a comprehensive evaluation of PPA on privacy concerned tasks, in particular, online shopping (i.e., Products-10K) and selfies sharing (i.e., RAF-DB) in addition to the MNIST and CIFAR10 based extensive validations. Experimental results affirm that PPA can accurately infer the preference of user datasets in FL, including majority/minority class, and top- k (e.g., $k = 2, 3$) contingent on a local user’s characteristics. Our experiments demonstrate that the PPA retains high efficiency when the number of users in FL and the number of local training epochs adopted by the user increase. We evaluate the PPA against the defences of dropout [41] and differential privacy [12], resulting in the conclusion that the PPA is still highly effective.

2 BACKGROUND AND RELATED WORK

In this section, we first introduce FL as well as its aggregation mechanism FedAvg, and then briefly describe existing known inference attacks.

2.1 Federated Learning

The FL fundamentally obviates the problematic raw data sharing from distributed users to a centralized server to train or update the global model. In FL, each user trains local model and uploads merely the model rather than any raw data to the server for computing each new round of global model. FedAvg [29] is the most well-known aggregation mechanism adopted by FL. In FedAvg, the global model θ_{agg} in round t is computed as follows:

$$\theta_{agg}^t = \sum_{n=1}^{N_{user}} \frac{D_n}{D} \theta_n^t, \quad (1)$$

where N_{user} users participating in FL, each holding D_n data points to train local model θ_n^t in round t . In addition, FedAvg usually utilizes a parameter C : the fraction of users that participate in aggregation at a given round. This is useful considering the ‘straggler’ due to network stability or simply leaving of some users. When the sampling rate C is set to 0.1-0.2, the FL is already able to strike a good balance between computational efficiency and convergence rate, as demonstrated by [29]. Therefore, for the selective aggregation experiments in our work, we align previous work [29] by normally setting the proportion of participated users at each aggregation (i.e. $k = 1-4$ if $N_{user} = 10$) in order to obtain the best experimental effect.

2.2 Membership Inference Attack

The membership inference attack [39] proposed by Shokri *et al.* constructs shadow models by imitating the behavior of target model, and then trains the attack model according to their outputs, which can infer the existence of specific data in the training set. Salem *et al.* [38] optimized the attack by decreasing the number of shadow models from n to 1. Nasr *et al.* [32] designed a white-box membership inference attack against centralized and FL by exploiting the vulnerability of stochastic gradient descent algorithm. Zari *et al.* [54] also researched the passive membership inference attack in FL. Chen *et al.* [8] provided a generic membership inference attack to attack the deep generative models and judged whether the image belongs to the victim’s training set by combining the proposed calibration technology. Leino *et al.* [23] utilized the impact of model overfitting to design white-box membership inference attack, and demonstrated that this attack outperforms prior black-box methods. Pyrgelis *et al.* [36] focused on the feasibility of membership inference attacks on aggregate location time-series, and use adversarial tasks based on game theory to infer membership information on location information. Some membership inference attacks [16, 17, 19] are devoted to the attack generative model under the white-box and black-box settings.

2.3 Property Inference Attack

Ganju *et al.* [13] found that fully connected neural networks are invariant under permutation of nodes in each layer and developed a property inference attack that can extract property information from the model. Melis *et al.* [30] devised a feature leakage attack in collaborative learning that can infer properties that hold only for a subset of the training data and are independent of the properties that the joint model aims to capture. Recently, Mathias *et al.* [34] studied the impact of model complexity on property inference attacks in convolutional neural networks and the results demonstrated that the risk of privacy leakage exists independently of the complexity of the target model. Gopinath *et al.* [14] proposed a property inference attack that automatically infers formal properties of feed-forward neural networks. They use encoding convex predicates on the input space to extract the input properties.

2.4 GAN Attack

Hitaj *et al.* [18] first proposed GAN attack against FL. The attacker disguises as a normal user to join the model training and obtains the imitation data of other participants based on GAN to infer

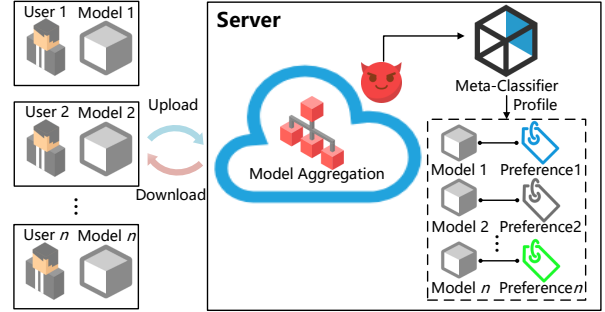


Figure 2: Threat model of PPA.

the privacy information. In addition, Wang *et al.* [47] proposed an inference attack based on GAN and multitask discriminator in FL, which achieves user privacy disclosure and is able to recover the private data of the target user on the server-side without interfering with the training process.

2.5 Privacy Inference Attacks on FL

In FL, there have been great efforts to explore its privacy leakage through various inference attacks, including membership inference [32, 54], property inference [30] and GAN [18, 47]. These inference attacks can obtain a variety of user privacy information from the upload model. However, no attack reveals that the *preference classes* in user dataset can be inferred. Therefore, our PPA is positioned as a new type of privacy inference attack orthogonal to known ones.

3 PREFERENCE PROFILING ATTACK

In this section, we first define the threat model and clarify the attack goals, then present an overview of PPA, followed by PPA implementation details of each component. To ease the description and understanding, we mainly use majority class preference profiling for descriptions. But the attack is equally applicable to the minority class preference and further extendable to top- k classes preference profiling.

3.1 Threat Model and Attack Goals

3.1.1 Threat Model. There are two types of entities in FL: local users and a global server. Generally, the server is assumed to be malicious and launches PPA to profile a targeted user’s preference through observing the user’s uploaded model, shown in Figure 2. The capabilities and knowledge of both entities are elaborated as follows:

- **Victims/Users:** Victims are the users whose private local data preferences are interested by the server or attacker. Local users participate in FL and collaboratively contribute to learning a global model without directly sharing their localized data. Due to statistical heterogeneity, they have different data volumes per class, thus forming diverse data distributions. We assume that users neither trust other users nor share local data and model parameters with each other. Users genuinely follow the FL procedure and they may employ some common privacy-enhancement techniques, particularly differential privacy and dropout.

- **Attacker/Server:** The server intends to steal a victim’s preference, especially, majority information from her uploaded model, e.g., shops train the federated model based on users’ shopping records, while using the PPA to analyze users’ shopping habits. FL realizes privacy protection by local training instead of uploading sensitive data to the server. Therefore, in most inference attacks on FL [18, 30, 32], the server usually acts as an attacker trying to infer privacy information from the user upload model. We assume that the server knows the types of users’ training datasets and can obtain a small set of benign samples covering all categories, e.g., from public sources, as an auxiliary dataset. The auxiliary dataset does not need to intersect with any user’s training dataset. The assumption of accessible small public dataset in FL is essentially aligned with [6, 11, 32, 57]. We assume that the server purposely chooses a specific subset of local models to update the global model through *model aggregation*, which is a common FL technique to mitigate bad effects from ‘straggler’ users due to, e.g., unstable network or simply leaving [25, 26].

3.1.2 Attack Goals. Overall, PPA is a white-box attack, and the attacker can profile preferences of all participated users simultaneously. The attacker aims to achieve the following goals:

- **Attack Efficacy.** The PPA is to achieve a high attack success rate simultaneously for all users in FL, even if the user applies common privacy-preserving approaches (i.e., differential privacy and dropout).
- **Attack Stealthiness.** This is to ensure that the global model availability and utility are not degraded and its accuracy is on par with that trained via a normal FL without the PPA. Since the selective aggregation mechanism we designed does not forge models and disguised under the common sampling strategy, it is difficult for users to be aware that their local models are under attack as the model utility is not affected.
- **Attack Generalization.** This goal is to ensure that our attack is generic to diverse FL settings (e.g., heterogeneous data), task domains (e.g., image, textual) and varying preference profiling interests (e.g., most liked, most disliked, top- k with k no less than 1), number of FL users, and number of local training epochs chosen by individual users.

3.2 PPA Overview

The PPA is based on the key observation that sample proportion size of classes in the training dataset can have a direct impact on a model’s gradient change sensitivity. The server as an attacker exploits user model sensitivity extraction to profile user (data) preferred class(es), especially majority and minority class that to a large extent is most interested in commercial applications as we later evaluated. At the same time, the global model accessed by the user is provided without utility degradation while facilitating the PPA by selectively aggregating a subset of user models, namely selective aggregation. Overall, the PPA has four steps as illustrated in Figure 3, each of which is succinctly described below and then elaborated. The used notations are summarized in Table 1.

- (1) **User Local Model Training.** Users with heterogeneous data train models locally and upload them to the server.

Table 1: Notation Summary

Notation	Description
N_{user}	Number of users in FL.
mc_n	Majority/minority class in n th user’s local data.
T	Training rounds of FL.
θ_n^t	Local training model of user $_n$ in round t .
D_{aux}	Auxiliary dataset held by the server.
α	Learning rate when server extracts sensitivity.
m	Meta-classifier.
Agg()	Model aggregation operations.
k	Number of models selected for aggregation.
N_{label}	Number of classes in the dataset.
S_n^t	Model sensitivity of user $_n$ at round t .
DS_n^t	Differential model sensitivity of user $_n$ at round t .
Th_{round}	Discrimination round threshold.

- (2) **Extract Model Sensitivity.** After receiving a local user model, the server uses the auxiliary dataset to retrain the model in order to extract the model sensitivity per class.
- (3) **Profile User Preference.** When getting model sensitivity, the meta-classifier is used to predict a user preferred class(es).
- (4) **Selective Aggregation.** Instead of forming the global model through all user models, only k models with the highest/lowest model sensitivity of its majority/minority class are used in the aggregation of the targeted local model. And then this aggregated model is sent to the targeted user—each user may receive a different aggregated model. This is to improve the PPA attack accuracy.

Step (4) requires a meta-classifier, which is prepared during the offline phase. In other words, before the FL begins among multiple users, the server trains the meta classifier offline based on auxiliary dataset D_{aux} . The implementation details of each step and the offline meta-classifier training are elaborated in the following. According to the time sequence, we start by meta-classifier offline training.

3.3 Train Meta-Classifier Offline

Algorithm 1: Train Meta-Classifier in Centralized Learning

- 1 **Input:** Auxiliary dataset D_{aux} , learning rate α
- 2 **Output:** Meta-classifier m
- 3 Sample the data in D_{aux} into multiple data distributions and train shadow models respectively
- 4 Record i th shadow model parameters θ_{shadow_i} and its preference class mc_i
- 5 Divide D_{aux} into N_{label} retraining datasets with all classes:

$$D_{aux} \rightarrow \{D_{aux_1}, \dots, D_{aux_t}, \dots, D_{aux_{N_{label}}}\}$$
 with D_{aux_t} having samples solely from the t th class.
- 6 Record retrained model parameters $\theta_{retrain_i}$ and compute model sensitivity S of its preference class

$$S = \sum |(\theta_{retrain_i} - \theta_{shadow_i}) \cdot \frac{1}{\alpha}|$$
- 7 Label the meta data (S, mc_i) , and train meta-classifier m

Before FL begins, the server needs to train a meta-classifier with the auxiliary dataset D_{aux} , as detailed in Algorithm 1. Firstly, the server samples the data in D_{aux} into a subset to resemble a heterogeneous data distribution of a user. The sampling repeats a

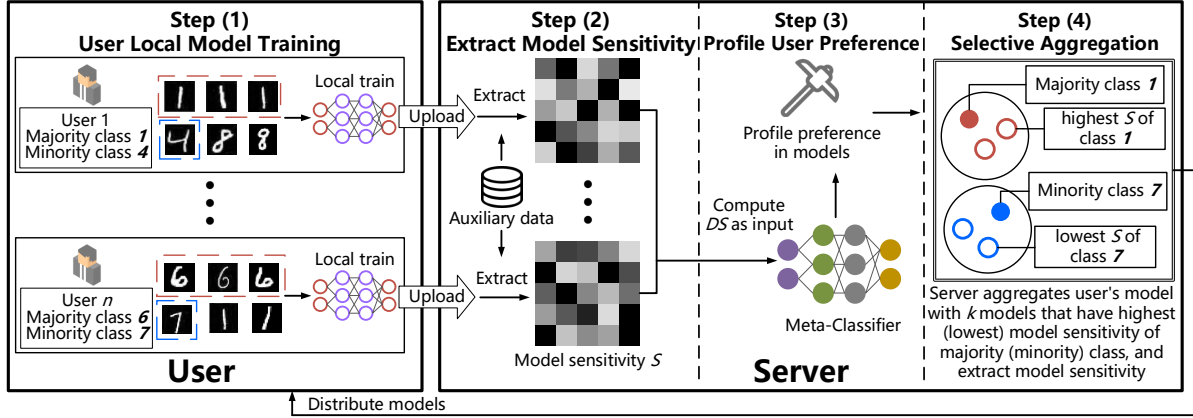


Figure 3: An overview of PPA.

Algorithm 2: Train Meta-Classifier in Federated Learning

- 1 **Input:** Auxiliary dataset D_{aux} , learning rate α
- 2 **Output:** Meta-classifier m
- 3 Combine the data in D_{aux} into multiple data distributions and train shadow models respectively
- 4 Record preference class mc of each shadow model
- 5 Divide D_{aux} into N_{label} retraining datasets with all classes: $D_{aux} \rightarrow \{D_{aux_1}, \dots, D_{aux_t}, \dots, D_{aux_{N_{label}}}\}$ with D_{aux_t} having samples solely from the t th class
- 6 **Shadow Model Pairing:**
- 7 Aggregate each shadow model with its paired one that has opposite preference class, and record the aggregated model parameters for such shadow model θ_{agg_i}
- 8 Retrain θ_{agg_i} on per class subset D_{aux_t} to record model parameters $\theta_{agg_i}^{retrain}$
- 9 Compute model sensitivity of this aggregated model $S1 = \sum |(\theta_{agg_i}^{retrain} - \theta_{agg_i}) \cdot \frac{1}{\alpha}|$
- 10 **Shadow Model Updating:**
- 11 Update aggregated model θ_{agg_i} on dataset corresponding to the i th shadow model to resemble the local model training for the next round in FL, and record updated model parameters θ_{aux_i}
- 12 Retrain θ_{aux_i} on per class subset D_{aux_t} to record model parameters $\theta_{aux_i}^{retrain}$
- 13 Compute updated model sensitivity of its preference class $S2 = \sum |(\theta_{aux_i}^{retrain} - \theta_{aux_i}) \cdot \frac{1}{\alpha}|$
- 14 Label the meta-data $(|S1 - S2|, mc)$, and train meta-classifier m

number of times. For each subset, a shadow model is trained and its preferred class is acted as the label. Secondly, the server separates D_{aux} into N_{label} subsets $\{D_{aux_1}, \dots, D_{aux_t}, \dots, D_{aux_{N_{label}}}\}$ where N_{label} is the total number of classes, each subset consisting of samples from a single class. Then, each shadow model is retrained per subset (D_{aux_t}) to extract shadow model sensitivity per class. Thirdly, such sensitivity (in particular, the gradient change) and its preferred class given a shadow model are used as the training set to train the meta-classifier. The meta-classifier can profile the preference class of the dataset.

However, the meta-classifier trained in the above straightforward manner is only suitable for centralized deep learning not the collaborative learning, in particular, in FL. Because when a local model is aggregated, the data distribution characteristics will be concealed within the global model, resulting in the model sensitivity fading of each user preference class in the following round. To overcome this challenge, we improve Algorithm 1 to make the meta classifier applicable to FL, as detailed in Algorithm 2. Generally, we leverage two specific improvements: paired aggregation, and differential sensitivity in two consecutive rounds.

In the meta-classifier training of FL, each shadow model will be paired with another shadow model. The steps are as below.

- (1) For the i th shadow model with majority class mc_i , the server selects the other shadow model with the highest model sensitivity of mc_i from all rest shadow models, and aggregates it with the i th shadow model.
- (2) The server extracts the model sensitivity of the aggregated model $S1$, and updates each aggregated model on the dataset corresponding to each shadow model.
- (3) Then the model sensitivity $S2$ of the updated i th shadow model in the next round is extracted.
- (4) The difference between $S1$ and $S2$ resembling two consecutive rounds in FL, $|S1 - S2|$, and its preferred class are used to train the meta-classifier in FL.

Note in step (1), in the case of minority, the model with the lowest model sensitivity of mc_i model is selected for pairing. Also, the $S1$ is extracted from the aggregated model, while the $S2$ is merely extracted from the updated local model.

The meta-classifier will be used to accurately profile the user's preference during the FL learning procedure when the sensitivity of user uploaded model is extracted and fed. The input of meta-classifier is the model sensitivity difference of two consecutive rounds ($|S1 - S2|$). In order to maximize the differential model sensitivity and make the meta-classifier get more accurate classification, we propose and leverage selective aggregation during the FL training, which will significantly increase $S1$. Since $S2$ remains relatively unchanged regardless of whether the selective aggregation is employed, a higher differential model sensitivity will be generated in the next round to obtain accurate profiling.

3.4 User Local Model Training

The FL is with a number of users in practice, and those users may locate in different regions with statistical and system heterogeneity. The PPA concerned statistical heterogeneity could be a result of data collected being personalized [55]. Thus, each user's training set has its own preferred category/class. As shown in step (1) in Figure 3, each user local data thus has its unique data distribution. Each user has a majority/minority class mc_n , that is, the largest/lowest number of samples in the dataset. For example, label 1 and label 6 are the majority classes of user₁ and user_n, and label 4 and label 7 are the minority classes of user₁ and user_n, respectively, as exemplified in Figure 3. In FL, the local model may be trained multiple epochs before it is uploaded to the server in an FL round. Our PPA has naturally tolerated such variation, which is invariant to the epoch number adopted by the user (see Section 4.5.2). After local training, each user updates the model parameter θ_n^t and uploads it to the server at the t_{th} round. The local model inadvertently memories the preference of the corresponding user, which is the information that the meta-classifier wants to profile later.

3.5 Extract Model Sensitivity

To quantify the model sensitivity to preference class, we utilize sum of absolute values of the gradient changes before and after the local user model retraining, which is expressed:

$$S = \sum \left| \frac{\delta}{\delta \theta_n^t} L(\theta) \right| = \sum \left| (\theta_n^t - \theta_n^{t'}) \cdot \frac{1}{\alpha} \right|, \quad (2)$$

where θ_n^t and $\theta_n^{t'}$ respectively represents the uploaded and retrained model parameter vector of user_n at the t_{th} FL round, and $L(\cdot)$ represents the loss function. Given a local model uploaded, the server re-trains it based on the retrain dataset $\{D_{aux_1}, \dots, D_{aux_t}, \dots, D_{aux_{N_{label}}}\}$ to extract the sensitivity of the model per class. The $\theta_n^{t'}$ denotes the retrained model. The process is detailed in Algorithm 3.

3.6 Profile Preference Class

We launch the PPA in the FL training phase. In this phase, the server leverages a trained meta-classifier to profile user preference after extracting its uploaded model sensitivity. The meta-classifier profiles preference classes based on the differential model sensitivity between consecutive rounds. There are two considerations we take to improve the attacking accuracy.

Firstly, it may be inaccurate to determine the user's preference class merely according to sensitivity extracted from one FL round. Therefore, we determine the preference based on a number of consecutive rounds only if their preferences predicted by the meta-classifier are all same. This number of rounds is denoted as Th_{round} . Given meta-classifier outputs the same preference of a user in consecutively Th_{round} FL rounds, this preference is locked, and the PPA against this user is completed, which means the monitoring on this user is no longer needed. The process is detailed in Algorithm 4.

Secondly, the FL aggregation is always a hinder to inference attacks [30, 32]. This is a result of learning global model merging all users' data characteristics. In this context, after one and more FL rounds, data characteristic of a given user is concealed and faded. The PPA is prevented from extracting user's model sensitivity accurately reflecting the corresponding local data characteristics

Algorithm 3: Extract Model Sensitivity of Class c

```

1 Input: Local models of usern in the round  $t$   $\theta_n^t$ , Auxiliary
   dataset  $D_{aux}$ , learning rate  $\alpha$ 
2 Output: Model sensitivity of class c  $S_n^t$ 
3 Set  $S_n^t = 0$ 
4 Generate retraining set of class c:  $D_{aux_c}$ 
5 foreach  $\theta_n^t$  from 1 to  $N$  in the round  $t$  do
6   Retrain model  $\theta_n^{t'} = \theta_n^t.train(D_{aux_c}, \alpha)$ 
7   foreach neuron  $i$  in  $\theta_n^{t'}$  do
8     Compute  $S_{(n,i)}^t = \left| (\theta_n^t - \theta_n^{t'}) \cdot \frac{1}{\alpha} \right| = \left| \frac{\delta}{\delta \theta_i} L(\theta) \right|$ 
9      $S_n^t += S_{(n,i)}^t$ 
10  end
11 end

```

and achieving higher PPA accuracy. To circumvent this issue, we propose the selective aggregation elaborated as follows.

Algorithm 4: Profile Preference Class

```

1 Input: Model sensitivity  $S_n^t$  of usern in the round  $t$ , Model
   sensitivity  $S^{t-1}$  of aggregated model in the last round  $t-1$ ,
   Round threshold  $Th_{round}$ 
2 Output: Preference class of usern  $mc_n$ 
3 Users train locally and upload models  $\theta_n^t$ 
4 Server retrains  $\theta_n^t$  based on retraining dataset to get  $\theta_n^{t''}$ 
5 Extract model sensitivity  $S_n^t$  of  $\theta_n^t$ 
6 Compute the differential model sensitivity between  $S_n^t$  and  $S^{t-1}$ 
   resembling two consecutive rounds  $|S^{t-1} - S_n^t|$ 
7 Input differential model sensitivity into meta-classifier, and profile
   preference class  $mc$ 
8 if same result in  $Th_{round}$  rounds then
9   | PPA against this user is completed
10 end
11 Each uploaded model of user is aggregated with  $k$  models that have
   the highest/lowest model sensitivity of its majority/minority class
12 Extract model sensitivity  $S^t$  of each aggregated model and then
   transfer back to corresponding user

```

3.7 Selective Aggregation

There are two challenges of selective aggregation confronted by the PPA: 1) how to prevent the user model sensitivity from being decreased or canceled by the global aggregation process after a number of FL rounds? 2) how to further amplify the user model sensitivity to reflect the user's specific local data characteristics?

In the selective aggregation, given a targeted user, the server selects models of k users who exhibit an opposite majority/minority class as their models have the opposite highest/lowest extracted model sensitivity—note lowest sensitivity corresponds to majority class. Then these $k+1$ models are aggregated to form a joint model, which is then sent back to the targeted user only, as shown in Figure 4—for other users who are not interested by the attacker, the joint model sent to them follows a normal aggregation. After selective aggregation, the server extracts the model sensitivity of each aggregated model for the next round of meta-classifier profiling. The selective aggregation is inconspicuous to the local users due to two main facts. Firstly, users only communicate with the server rather than other users and the communicated data is merely the

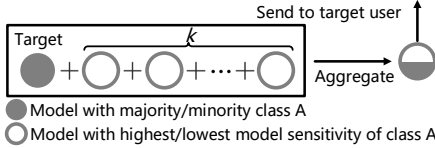


Figure 4: Selective aggregation. The selected k users have opposite model sensitivity of class A that is the majority/minority class of the targeted user.

uploaded local model and the downloaded joint model. Secondly, it is a common practice of only sampling a subset of local models in FL for aggregation to mitigate bad consequences from straggler participants [25, 26]. Therefore, it is tractable to make the users unaware of selective aggregation. Later we experimentally show that the local data accuracy predicted by the global model is similar from the user's perspective with and without implementing the selective aggregation.

The input of meta-classifier is the model sensitivity difference of two consecutive rounds. We define it as differential model sensitivity (DS), and compute as follows:

$$DS_n^t = |S_{agg_n}^{t-1} - S_n^t|, \quad (3)$$

where $S_{agg_n}^{t-1}$ is the model sensitivity of the *aggregated model* in round $t-1$, and S_n^t is the model sensitivity of the updated user model in round t . Through selective aggregation, $S_{agg_n}^{t-1}$ of each model will be amplified, while the S_n^t is stable compared to the case without the usage of selective aggregation. Therefore, the DS in each round is greatly improved since the meta-classifier is trained based on DS , the larger the DS , higher the profiling accuracy.

4 EXPERIMENTS

In this part, we experimentally evaluate the PPA and analyze its attack performance under four data heterogeneity metrics(CP, CD, UD , and ID) in FL. In addition, we validate the effectiveness of selective aggregation under a number of varying settings. Moreover, the scalability of the PPA is examined and validated.

4.1 Experimental Setup

In our experiments, common personal computers act as users in FL with an identical configuration (as system heterogeneity is not our concern): Intel Core i5 processors for a total of four cores running at 3.20 GHz and 12 GB RAM. We use H3C UIS 3010 G3 8SFF server as the FL aggregator that is the attacker, which is equipped with two Intel Xeon CPU Silver 4214, 128 GB RAM and two 480 GB SSD.

To evaluate the efficacy of the PPA inference, we conduct experiments on four different datasets spanning from image to textual domains. In particular, the Products-10K is used to represent a commercial scenario and the facial expression dataset RAF-DB represents personal concern about his/her private information.

4.1.1 Dataset. We select four datasets to evaluate PPA. MNIST and CIFAR10 are used to comprehensively show PPA performance under four data heterogeneity metrics and the effectiveness of selective aggregation. Products-10K and RAF-DB are real-world datasets used to indicate PPA performance under commercial scenarios of shopping and social network and the scalability of PPA.

- **MNIST** is an image dataset of handwritten numbers from 0 to 9 [22]. The images in the database are all 28×28 grayscale images, including 60,000 training images and 10,000 test images.

- **CIFAR10** is an image dataset for the recognition of universal objects [21]. There are 10 categories of RGB color images with size of is $32 \times 32 \times 3$. It consists of 50,000 training and 10,000 testing samples, respectively.

- **Products-10K** is a product identification set built by JD AI research, which contains about 10000 products often purchased by Chinese consumers and covers many categories, e.g., fashion, food, health care, household products, etc [3]. We use this dataset to resemble a real-world FL shopping scenario and evaluate the impact of our attack.

- **RAF-DB**, Real-world Affective Faces Database [24], is a large-scale facial expression database with around 30K great-diverse real-world facial images. Images in this dataset are of the great variability in subjects' age, gender and ethnicity, head poses, lighting conditions, occlusions, post-processing operations, etc.

4.1.2 Data Distribution Metrics. Four metrics defined below are used to resemble the statistical heterogeneous of the local user data in FL. Generally, the first two metrics are utilized to evaluate PPA performance under a varying data distribution given a user, and the last two are used to validate the applicability of the selective aggregation.

- **Class Proportion (CP)** represents the proportion of each class in the user dataset. Closer the value to 1, more samples in this class. The CP is expressed as:

$$CP = \frac{\# \text{number of samples given a class}}{\# \text{dataset size}} \quad (4)$$

- **Class Dominance (CD)** represents the dominance of a class in the user dataset. The numerator is the difference between the majority/minority number and the class closest to it, expressed as below:

$$CD = \frac{\# |\text{Majority/Minority} - \text{Secondary}|}{\# \text{dataset size}} \quad (5)$$

- **User Dispersion (UD)** represents the divergence of preferred majority classes among users in FL. Numerator is the maximum difference in the number of users with the same preference class. Take an example to ease the understanding, there are three classes: A, B, C. Out of a total of 10 users there are 5 users with A as the preference class, 3 with B and 2 with C. The $UD = (5 - 2)/10 = 30\%$. The numerator in this case is $5 - 2 = 3$ and the denominator is 10. The closer the UD to 1, the more consistent the user preferences in FL, expressed as below:

$$UD = \frac{\# \text{range(user number)}}{\# \text{user number}} \quad (6)$$

- **Imbalance Degree (ID)** represents the degree of user data heterogeneity in FL, and measures the variance of local user *total* dataset volume/size. More specifically, different users have different number of local samples, e.g., user A having 1,000 and user B having a differing 2,000. A larger value means a greater variance of user data volume and a higher degree of data heterogeneity, computed as follows:

$$ID = \# s^2 (\text{user dataset volume}) \quad (7)$$

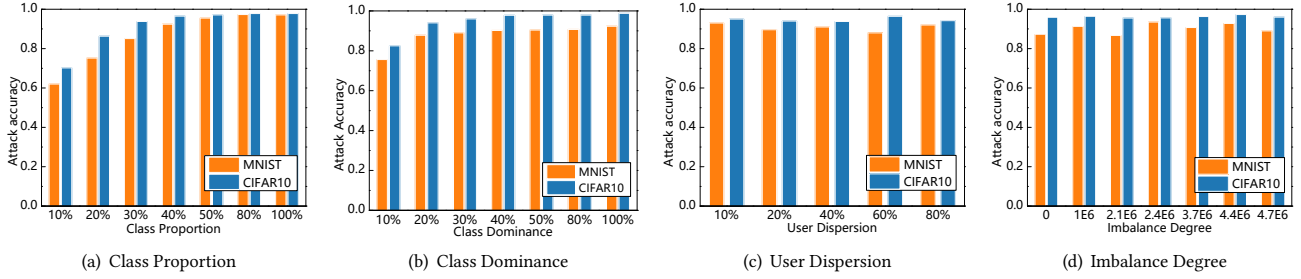


Figure 5: Attack accuracy of PPA under different metrics.

4.2 Attack Performance

Here, we use CIFAR10 and MNIST datasets for extensive PPA performance evaluations under each of the aforementioned metrics. The PPA is mainly evaluated against majority class. If the majority class predicted by meta-classifier is not the true majority class of the targeted user, *even the second majority class*, we all strictly regard that the PPA fails. It should be noted that in practice, inferring the second majority class is still valuable for the attacker, e.g., the most and the second most popular items of a shopping mall.

For all experiments unless otherwise specified, we set up a total number of 10 users in FL. Each local dataset has 4000 samples. We conduct multiple evaluations under the four metrics to entirely include the general data distribution in FL [29, 30, 32]. As for the server, it has 150 auxiliary samples per class that are non-overlapped with any user. During the PPA, the server applies selective aggregation (we compare it with normal aggregation in Section 4.3).

4.2.1 Attack Accuracy under CP. We decrease the *CP* from 100% to as low as 10%. A higher *CP* means that the preferred class has a larger number of samples, thus increasing the model sensitivity gap between this majority class and the rest classes. Therefore, the attack accuracy would be improved because of easier differentiating the majority class by the meta-classifier. The results of MNIST and CIFAR10 are displayed in Figure 5 (a), which do confirm this tendency. Meanwhile, CIFAR10 performs better than MNIST because the variation in model sensitivity becomes larger as the dataset becomes richer in features. Both cases' accuracy is beyond 90% when the *CP* is higher than 40%.

4.2.2 Attack Accuracy under CD. Here we vary the *CD* from 10% to 100% and the PPA results of MNIST and CIFAR10 are detailed in Figure 5 (b). When *CD* is close to 0%—the number of majority class is close to that of second majority class, the PPA accuracy of the majority class is low. This is because the model sensitivity extracted for majority and second majority classes are similar, making the meta-classifier to be confused to determine the truth one. Nonetheless, as *CD* increases, the attacking accuracy greatly improves.

From the experimental results under *CP* and *CD*, we can see that the presented PPA can effectively attack a user model preference within a wide range of data heterogeneity. In addition, richer characteristics of the data (i.e., CIFAR10) indicate a more effective meta-classifier for performing PPA.

Table 2: PPA Attack Accuracy vs Model Utility

Dataset	Attack Accuracy		Model Utility	
	Train	Test	Before Attack	After Attack
MNIST	0.994	0.894	0.913	0.902
CIFAR10	0.981	0.967	0.821	0.813

4.2.3 Attack Accuracy under UD. *UD* indicates the degree of variation in the preferences of different user groups, reflecting the overall trend of preference categories in FL. It may affect the selection of user models in each round of selective aggregation, thus we evaluate the relationship between different *UD* and attack accuracy, as shown in Figure 5 (c). Whether the group preference is more consistent (*UD* close to 1) or more discrete (*UD* close to 0), PPA can accurately profile the preference class of each individual in FL.

4.2.4 Attack Accuracy under ID. To affirm that selective aggregation is suitable for FL under heterogeneous data, we evaluate the performance of PPA as a function of varying *ID*, as shown in Figure 5 (d). The experimental results indicate that the data amount owned by a user does not affect the effectiveness of PPA.

Through the evaluations under *UD* and *ID*, the scalability of selective aggregation leveraged by PPA is validated.

4.2.5 Local Data Size and Class Number. In previous experiments, the local data size and number of classes in the local dataset are constant to be 4000 and 10, respectively. We here vary these two parameters (*CP* is retained as 40% and *CD* is retained as 50%). Specifically, for user data volume, we vary it from 2000 to 4000 by a step of 500. For the number of classes owned by a user, we vary it from 1 to 9 with a step by 2. We repeat 10 times for each setting. The attacking accuracy is shown in Figure 6. The results indicate that PPA performance is independent of the number of classes of local data. As for the local data size, it to some extent influences the PPA accuracy, especially when the sample itself (i.e., MNIST) is with a lower feature. However, the local data size has a very limited impact on attacking accuracy given that the CIFAR10 is with richer features.

4.2.6 Attacking Accuracy vs Model Utility. To be stealthier, the global model utility downloaded by the user should not be affected by the PPA. Otherwise, the user may be aware of the abnormality during the FL participation such as deviated model accuracy/utility resulted from the selective aggregation. In this context, we evaluate the user model utility (i.e., its accuracy) in each round. In addition, we summary the attack performance. As

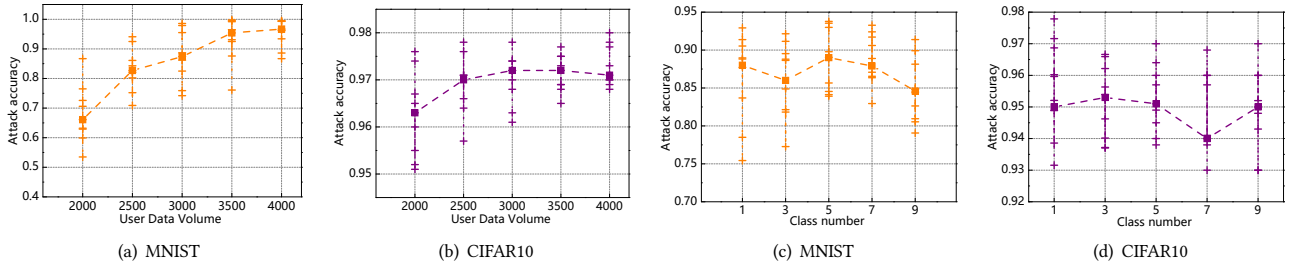


Figure 6: Attack accuracy of PPA against models trained on MNIST and CIFAR10 datasets. Figure (a) and (b) reveal the attack accuracy with different amounts of data. The median values are connected across different training set sizes. Figure (c) and (d) reveal the accuracy of the attacks with different number of classes.

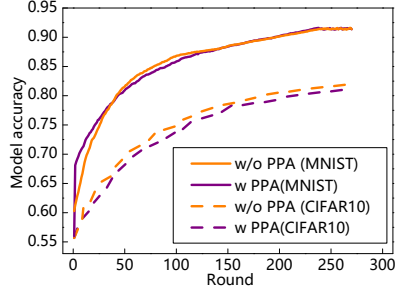


Figure 7: A comparison of model usability w/o the attack.

summarised in Table 2 (CP is 40% and CD is 50%), for attacking performance, we evaluate the training and testing accuracy of meta-classifier. For model utility, we compare the accuracy of the user’s local model before uploading in each round with the accuracy of the received aggregation model (after attack) in the following round. The experimental results show that given the often heterogeneous data distribution, PPA has the attacking accuracy of 0.894 and 0.967 in MNIST and CIFAR10. Most importantly, there is no notable model utility difference before and after attack (specifically, the applied selective aggregation), which obviates the user’s awareness of the PPA by solely examining the model utility. We also compared the change of user model accuracy with the number of rounds with and without the attack, as shown in Figure 7. The experimental results reveal that there is no difference in user model accuracy between the two cases because PPA does not tamper with the user model parameters. Therefore, the model with PPA does not differ so dramatically in accuracy from normal FL that may raise suspicion among users, which satisfies attack stealthiness.

4.3 W/O Selective Aggregation

So far, all experiments are with selective aggregation. We have not demonstrated the efficiency of the selective aggregation compared to the case when the selective aggregation is not leveraged. The latter means that a common aggregation algorithm, FedAvg, is used. In the following, we compare the PPA performance with/without selective aggregation from four aspects.

4.3.1 Differential Model Sensitivity. Each round of FL consists of two steps: model aggregation by server and local model updating by user. In each step per round, we extract the model sensitivity of

the majority class under selective aggregation and FedAvg aggregation respectively, as shown in Figure 8(a) and (b). Then, we also compare the differential model sensitivity under two aggregations, as shown in Figure 8(c) and (d).

As can be seen from Figure 8 (a) and (b), each round of selective aggregation (marked as avg) increases the model sensitivity. Then the next round of local training draws down the model sensitivity again. Though the model sensitivity of the *user uploaded model*, S_{agg_n} , under FedAvg aggregation has no notable difference from the selective aggregation method. The model sensitivity of the aggregated model, $S_{agg_n}^{t-1}$, does have a larger difference. Since $DS_n^t = |S_{agg_n}^{t-1} - S_n^t|$, the DS_n^t of selective aggregation method is greatly amplified compared to that of the FedAvg aggregation method, which can be clearly observed from Figure 8(c) and (d) that the DS_n^t of selective aggregation method is always above that of the FedAvg.

4.3.2 Attack Performance Comparison. Figure 9 indicates the accuracy comparison of PPA under federated model aggregation FedAvg [29] and selective aggregation, respectively. We set up 5 cases under two model aggregation methods. In the experiments, there are 10 users in FL, each user has 6000 samples, the server has 150 samples per class, CP and CD are randomly selected from 40% to 60%, and $k = 4$ in selective aggregation. The experimental results confirm that our attack has higher accuracy under the selective aggregation approach compared to the FedAvg. The reason is that the meta-classifier profiles the preference class according to DS . Compared with FedAvg, selective aggregation can improve DS in each round and make the meta-classifier perform better.

4.3.3 Selection of Value k . Here we evaluate the PPA performance as a function of k that is the number of models chosen in the selective aggregation (recall Figure 4). In the experiments, total number of uses is 12 and each user has 4,000. The PPA attack accuracy with k from 1 to 11 is depicted in Figure 10. We can see that the attack is most effective when k is 1-4, and then the attack success rate decreases as the number of aggregated models increases. This is not difficult to understand, using an extreme case, when $k = 11$, selective aggregation is equal to the common FedAvg aggregation, and the attack success rate largely depends on the data distribution of specific users in FL, as shown in Figure 9. In other words, the PPA attack accuracy for a given user under FedAvg aggregation is difficult to control, as the user’s model sensitivity is solely dependent on its local data characteristics, where the attacker has

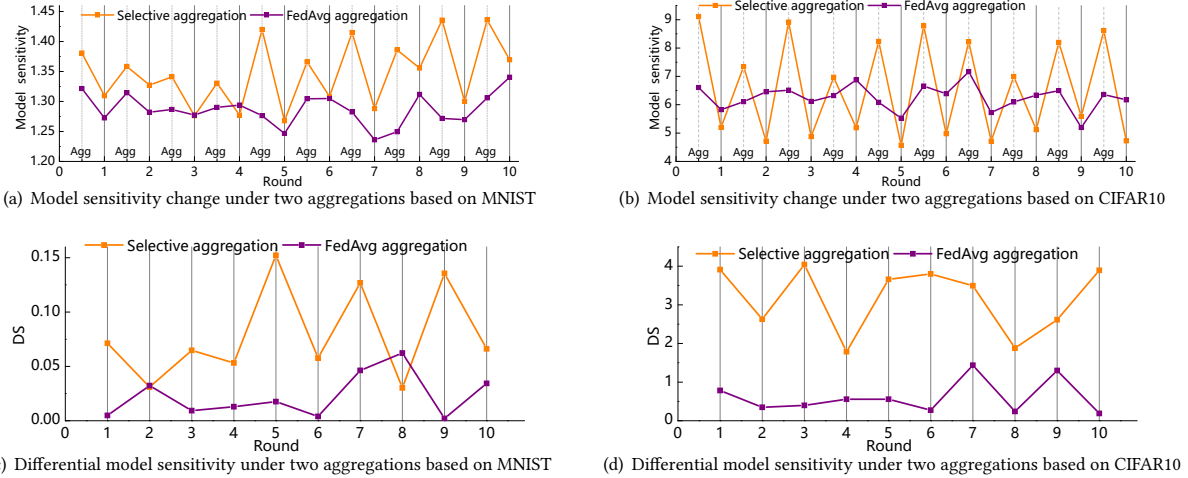


Figure 8: Model sensitivity change and differential model sensitivity under two aggregations.

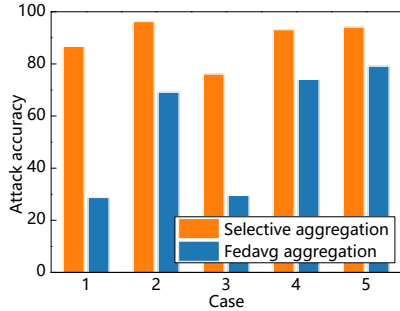


Figure 9: PPA performance under common Fedavg aggregation and the presented selective aggregation.

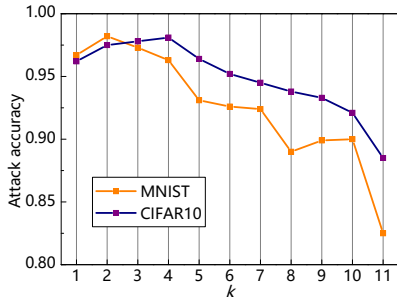


Figure 10: The relationship between k in selective aggregation and attack accuracy.

no other means to improve its model sensitivity opposite to the selective aggregation. The intuitive aggregation of models renders less preference sensitivity change, thus making the meta-classifier more difficult to accurately profile the preference. In this context, the value of k should be properly selected according to the scale of users in FL in order to achieve optimal attacking performance.

4.4 Real-World Case Studies

Beyond the aforementioned MNIST and CIFAR10 tasks, we leverage two more case studies to resemble real-world threats posed by the

Table 3: PPA in Practical Scenes

Scene	Preference Class	PPA Output	Attack Accuracy
Shopping Scene (Products-10K)	top1-(Food)	top1-(Food)	0.78
	top2-(Food, Clothing)	top2-(Food, Cosmetics)	0.78
	top3-(Food, Clothing, Cosmetics)	top3-(Food, Cosmetics, Clothing)	0.88
Social Network (RAF-DB)	top1-(Disgusted)	top1-(Disgusted)	0.88
	top2-(Disgusted, Neutral)	top2-(Disgusted, Neutral)	1.00

PPA. In the first case, the PPA attempts to profile popular sale items. In the second case, the PPA infers the user emotions. Note here we further profile the top- k preference classes, including majority and minority classes. Because top- k preference classes already contain sufficient privacy information about user data distribution in real scenes. Consequently, we evaluate the top- k output from the meta-classifier, and the results are summarized in Table 3. Experimental details are described below.

Note the top- k accuracy here is relatively different from the one usually used in image classification tasks. The top- k predicted classes are exactly the same as the top- k ground-truth classes, but without caring the ranking order of these k classes. For instance, the ground-truth preferred classes are A, B, C, D, E in descending order. We regard that predicted cases of $\{(A, B, C), (A, C, B), (B, A, C)\}$ in order are all acceptable and correct in our top- k setting.

4.4.1 Case I – Customer Preference Profiler. We resemble an FL scenario based on shopping records of Products-10K dataset, which contains 10 shops, each with 4000 shopping records. The CP is 35% and CD is 32.5% in the experiment, and the server has 1500 auxiliary set data. These shops are collaboratively training a joint model. In the experiment, we randomly select a shop for PPA and profile its shopping preference (i.e., most sale items that could be privately concerned). We extract the top- k (i.e., $k = 2, 3$) preferences of its local setting. The experimental results are shown

Table 4: PPA Performance under Different User Numbers

User Number	Attack Accuracy
10 users in FL	0.894
50 users in FL	0.82
100 users in FL	0.832

in Table 3. Among the shopping records of the customer we attack, the top-3 classes are Food, Clothing and Cosmetics. The final outputs of PPA are Food, Cosmetics and Clothing, and the attack accuracy is 78%. It can be seen that without considering the top-3 order, PPA can infer customers' shopping habits with 78% attack accuracy. Therefore, the server can successfully infer popular items, then push relevant advertisements or give this information to its competitor.

4.4.2 Case II – User Psychological Profiler. In this experiment, the dataset of RAF-DB is used, and the CP is 67.5% and CD is 62.2%. The server intends to infer the personality hidden in the expression model published by users on social networks. For example, when PPA finds that photos of negative emotions dominate in the model uploaded by users, it can speculate that the user's personality may be negative. The experimental results are shown in Table 3. In the photo gallery of the users we attack, the two most common expressions are disgust and neutrality. Then we can infer that the target user's personality tends to be negative. When users normally use their photos for training in FL, PPA can potentially profile the psychological character.

4.5 Scalability of PPA

We further investigate three crucial factors relevant to the scalability of the PPA in FL. The first is the number of users or participants, where most previous experiments use value of ten. The second is the local training epochs, where all previous experiments use default one local training epoch. The third factor is the size of the public auxiliary samples reserved by the attacker to facilitate the model sensitivity extraction.

4.5.1 Number of Users. The number of users in FL is increased from 10 to 50 and 100. This experiment is based on RAF-DB dataset, in which each user has 4000 training data, CP is 62.5%, CD is 57.5%, and 100 auxiliary sets per class. Under this setting, we attack seven users who have different preference classes. The experimental results are shown in Table 4. The result validates that the performance of PPA is insensitive to the user number, and the attack accuracy remains to be high, 83.2%, in the case of 100 users. This is mainly because selective aggregation will aggregate the victim model with other user models that are most conducive to the attack, regardless of the number of users.

4.5.2 Local Training Epochs. A local user can control the number of local training epochs being more than 1 before updating the local model to the server. Here we evaluate whether the PPA is insensitive to the the number of training epochs. In the experiments, RAF-DB is used as a training task and the auxiliary dataset is 150 per class. Each user has 3000 training data, and CP is 62.5% and CD is 56%. We first set training epoch to be 1, and randomly select 4 victim users to perform PPA. Then we increase the local training epochs to be 20. The PPA performance under 1 local training epoch and 20 local training epochs are detailed in Table 5. It can be seen

Table 5: PPA Performance under Different Training Epochs

Training Epoch	PPA Preformance	Average Accuracy
Epoch Num. = 1	User1: 0.92	0.88
	User2: 1	
	User3: 0.74	
	User4: 0.86	
Epoch Num. = 20	User1: 0.88	0.87
	User2: 1	
	User3: 0.72	
	User4: 0.88	

Table 6: PPA Performance under Different Numbers of Auxiliary Data

Auxiliary Dataset	Average Accuracy
20 per class	0.675
100 per class	0.819
150 per class	0.86

from the experimental results that when users increase the number of training epochs locally, the performance of PPA is merely influenced. There is a slight variance but without obvious tendency (i.e., the attacking accuracy of user 4 is increased due to variance). We can empirically conclude that the effectiveness of the PPA is independent of the epoch number of local training.

4.5.3 Auxiliary Data. The extraction of model sensitivity requires using a number of public auxiliary data. The more auxiliary data, the more comprehensive the sample features it contains, which will make the extracted model sensitivity close to the real situation. In this context, it is expected that the number of auxiliary data can affect the attack accuracy. We thus test PPA performance under different numbers of auxiliary data. The experiment setting is the same as the experiment of local training epochs. We just vary the number of auxiliary data available to the attacker and evaluate the attack accuracy under 20, 100 and 150 auxiliary samples per class, which experimental results are shown in Table 6. The results affirm that the more auxiliary sets, the better PPA performance. However, when there are few auxiliary sets (20 per class), our attack still has 67.5% accuracy (the guessing accuracy is 14.3%). According to our observation, PPA can perform well when the number of auxiliary sets is about 100 per class in our experiments.

5 DISCUSSIONS

We further discuss the insights of the PPA with more experimental details. In addition, we demonstrate the effectiveness of PPA even when common privacy protection mechanisms (in particular, differential privacy and dropout) are applied by local users.

5.1 The Rationale of PPA

Generally, we recognize that the user's model can remember the preference class (majority/minority class) of the dataset during training, and reflects it *in the form of gradient change*. The gradient value of neural network determines the convergence direction of the model, which is an important index to make the model tend to fit. We find that it can be exploited to infer whether the model is sensitive to certain data. To prove it, we have done a series of preliminary and detailed experiments, which are elaborated in the following.

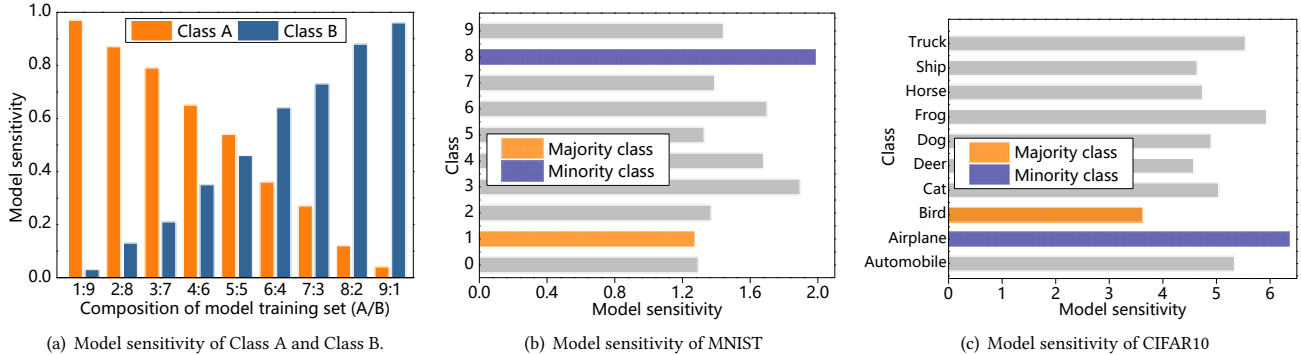


Figure 11: Model sensitivity change and extraction experiments.

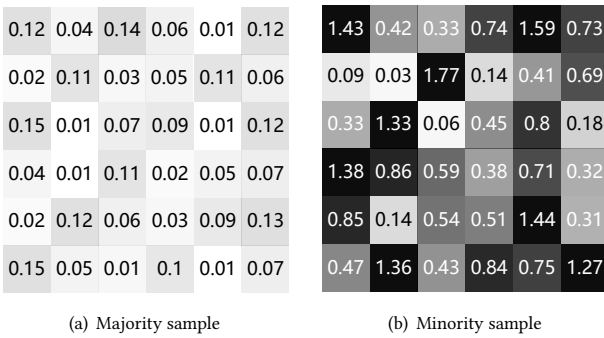


Figure 12: The gradient change of 36 randomly selected neurons after retraining by samples of the majority class (a) and minority class (b).

To simplify the investigation, we focus on a binary classification task. We change the data distribution of the training set of binary classifiers based on MNIST dataset, and extract the gradient change when they are later retrained by two kinds of samples A and B, respectively. Specifically, we firstly adjust the proportion of A and B in training set from 1:9 gradually to 9:1, and consequentially train 9 binary classifiers, in which the total amount of training sets of each model is 6000. After model training, we retrain the model with A and B samples respectively, and record the model sensitivity of class A and B between the two models, as shown in Figure 11 (a). The model sensitivity is linearly related to the sample size of the given class.

Beyond the simplified binary classification, we also extract model sensitivities for each class in the MNIST and CIFAR10 models, as shown in Figure 11 (b) and Figure 11 (c). In this experiment, we train two models based on MNIST and CIFAR10 datasets, respectively. The training set is a random sample of 6000 data to represent the data distribution of FL users. The majority class 1 and *Bird* account for 50%, minority class 8 and *Airplane* accounts for 2%, and the rest is evenly distributed. We affirm that the majority and minority classes correspond to the minimum and maximum values of the model sensitivity, respectively.

For further visualization, we extract the model sensitivity of majority and minority class in a model, by randomly selecting 36 neurons to show their gradient changes after retraining with a 6

Table 7: PPA Performance and User Model Utility under Defence Settings

	Task	No Def.	Drop.	ϵ -Differential Privacy				
				0.25	0.5	1	4	16
Attack	MNIST	0.89	0.85	0.76	0.87	0.88	0.88	0.89
	CIFAR10	0.97	0.96	0.94	0.96	0.96	0.97	0.97
Model	MNIST	0.90	0.87	0.89	0.89	0.90	0.90	0.90
	CIFAR10	0.80	0.62	0.67	0.78	0.79	0.79	0.79

$\times 6$ square grayscale plot. The larger the value of gradient change, the darker the color, as depicted in Figure 12. We can see that the gradient change is much smaller retrained by the majority class samples (Figure 12 (a)) than that by the minority class samples (Figure 12 (b)). The gradient value of neural network determines the convergence direction of the model, which is an important index to help the model fit, and can essentially reflect whether the model is sensitive to certain data distribution characteristics in our PPA. More specifically, each sample in the training set contributes to minimizing the model loss through stochastic gradient descent algorithm. For the data point(s) that does not exist or have a small amount in the training set, the model does not have a good generalization, especially, at the beginning of the model training, so this data point(s) will have a greater gradient effect to change the weights of the corresponding neurons to minimize the expected loss of the model. As a matter of fact, this is also an important motivation for taking model aggregation in FL: when users have various data distributions, the server can still make the global model converge to all data categories by aggregating all the local models. Thus, the natural data heterogeneity characteristic in FL is vulnerable to the presented preference inference attack.

5.2 When Our Attack Confronts Defenses

Dropout [41] and differential privacy [12] are two widely used techniques in the fields of formal verification [45], program synthesis [46] and deep learning privacy protection [44, 48, 53]. Here we investigate the attack accuracy and model utility when PPA is adopted in FL. The experimental results detailed in Table 7 demonstrate that the accuracy of PPA’s meta-classifier drops when a smaller privacy budget of ϵ of differential privacy is applied, and remains stable when the dropout is applied (i.e., CIFAR10). In the former case, even with a privacy budget as low as 0.25, our attacks still have a success rate up to 76% (guessing accuracy is 10%).

However, those protection mechanisms usually inevitably sacrifice utility (model accuracy), as we have evaluated and detailed in Table 7. It can be seen from the experimental results that the model utility/accuracy degrades: a higher protection level (smaller ϵ) means a lower model usability. Though the dropout and differential privacy can mitigate the user preference leakage to some extent, they come with a notable undesired utility trade-off.

6 CONCLUSION

This work uncovered a new type of privacy inference against FL that is the Preference Profiling Attack (PPA) to infer the preference classes of users. Based on our key observation that the gradient change reflects the sample size of a class in the dataset, we devised techniques to quantify and extract such change as model sensitivity to predict the preference class assisted with the meta-classifier. Extensive experiments indicated that the PPA is effective under various settings and poses real threats to preference sensitive applications in the real world, substantiated by two commercial applications. In addition, we have shown that the PPA can be well-scaled, which is insensitive to the number of FL participants and local training epochs employed by the user. Squarely applying common privacy protection cannot satisfactorily mitigate the PPA due to the unacceptable model utility degradation.

REFERENCES

- [1] Vito Walter Anelli, Yashar Deldjoo, Tommaso Di Noia, Antonio Ferrara, and Fedelucio Narducci. 2021. How to put users in control of their data in federated top-N recommendation with learning to rank. In *Proceedings of ACM/SIGAPP Symposium on Applied Computing*, SAC. 1359–1362.
- [2] Veruska Ayora, Flávio E. A. Horita, and Carlos Kamienski. 2021. Profiling Online Social Network Platforms: Twitter vs. Instagram. In *Proceedings of Hawaii International Conference on System Sciences*, HICSS. 1–10.
- [3] Yalong Bai, Yuxiang Chen, Wei Yu, Linfang Wang, and Wei Zhang. 2020. Products-10K: A Large-scale Product Recognition Dataset. *arXiv preprint arXiv:2008.10545* (2020).
- [4] Santiago Zanella Béguelin, Lukas Wutschitz, Shruti Tople, Victor Rühle, Andrew Paverd, Olga Ohrimenko, Boris Köpf, and Marc Brockschmidt. 2020. Analyzing Information Leakage of Updates to Natural Language Models. In *Proceedings of ACM SIGSAC Conference on Computer and Communications Security*, CCS. ACM, 363–375.
- [5] Kseniya Buraya, Aleksandr Farseev, Andrey Filchenkov, and Tat-Seng Chua. 2017. Towards User Personality Profiling from Multiple Social Networks. In *Proceedings of AAAI Conference on Artificial Intelligence*, AAAI. 4909–4910.
- [6] Xiaoyu Cao, Minghong Fang, Jia Liu, and Neil Zhenqiang Gong. 2021. FLTrust: Byzantine-robust Federated Learning via Trust Bootstrapping. In *Proceedings of Network and Distributed System Security Symposium*, NDSS.
- [7] Nicholas Carlini, Florian Tramèr, Eric Wallace, Matthew Jagielski, Ariel Herbert-Voss, Katherine Lee, Adam Roberts, Tom B. Brown, Dawn Song, Úlfar Erlingsson, Alina Oprea, and Colin Raffel. 2021. Extracting Training Data from Large Language Models. In *Proceedings of USENIX Security Symposium*, USENIX Security. 2633–2650.
- [8] Dingfan Chen, Ning Yu, Yang Zhang, and Mario Fritz. 2020. GAN-Leaks: A Taxonomy of Membership Inference Attacks against Generative Models. In *Proceedings of ACM SIGSAC Conference on Computer and Communications Security*, CCS. 343–362.
- [9] Prateek Chhikara, Prabhjot Singh, Rajkumar Tekchandani, Neeraj Kumar, and Mohsen Guizani. 2021. Federated Learning Meets Human Emotions: A Decentralized Framework for Human-Computer Interaction for IoT Applications. *IEEE Internet of Things Journal*, IoTJ, 8, 8 (2021), 6949–6962.
- [10] China. 2021. China Data Security Law. <https://www.china-briefing.com/news/a-close-reading-of-chinas-data-security-law-in-effect-sept-1-2021/>. Accessed Sep 21, 2021.
- [11] Ye Dong, Xiaojun Chen, Kaiyun Li, Dakui Wang, and Shuai Zeng. 2021. FLOD: Oblivious Defender for Private Byzantine-Robust Federated Learning with Dishonest-Majority. In *Proceedings of European Symposium on Research in Computer Security* ESORICS, Vol. 12972. 497–518.
- [12] Cynthia Dwork. 2006. Differential Privacy. In *Proceedings of Automata, Languages and Programming*, 33rd International Colloquium, ICALP, Vol. 4052. 1–12.
- [13] Karan Ganju, Qi Wang, Wei Yang, Carl A. Gunter, and Nikita Borisov. 2018. Property Inference Attacks on Fully Connected Neural Networks using Permutation Invariant Representations. In *Proceedings of ACM SIGSAC Conference on Computer and Communications Security*, CCS. 619–633.
- [14] Divya Gopinath, Hayes Converse, Corina S. Pasareanu, and Ankur Taly. 2019. Property Inference for Deep Neural Networks. In *Proceedings of IEEE/ACM International Conference on Automated Software Engineering*, ASE. 797–809.
- [15] Inken Hagedstedt, Mathias Humbert, Pascal Berrang, Irina Lehmann, Roland Eils, Michael Backes, and Yang Zhang. 2020. Membership Inference Against DNA Methylation Databases. In *Proceedings of IEEE European Symposium on Security and Privacy*, EuroS&P. 509–520.
- [16] Jamie Hayes, Luca Melis, George Danezis, and Emiliano De Cristofaro. 2019. LOGAN: Membership Inference Attacks Against Generative Models. In *Proceedings on Privacy Enhancing Technologies*. 133–152.
- [17] Benjamin Hiltrech, Martin Härtwich, and Daniel Bernau. 2019. Monte Carlo and Reconstruction Membership Inference Attacks against Generative Models. In *Proceedings on Privacy Enhancing Technologies*. 232–249.
- [18] Briland Hitaj, Giuseppe Ateniese, and Fernando Pérez-Cruz. 2017. Deep Models Under the GAN: Information Leakage from Collaborative Deep Learning. In *Proceedings of ACM SIGSAC Conference on Computer and Communications Security*, CCS. 603–618.
- [19] Hailong Hu and Jun Pang. 2021. Membership Inference Attacks against GANs by Leveraging Over-Representation Regions. In *Proceedings of ACM SIGSAC Conference on Computer and Communications Security*, CCS. 2387–2389.
- [20] Peter Kairouz, H Brendan McMahan, Brendan Avent, Aurélien Bellet, Mehdi Benni, Arjun Nitin Bhagoji, Kallista Bonawitz, Zachary Charles, Graham Cormode, Rachel Cummings, et al. 2019. Advances and open problems in federated learning. *arXiv preprint arXiv:1912.04977* (2019).
- [21] Alex Krizhevsky. 2012. Learning Multiple Layers of Features from Tiny Images. (2012).
- [22] Yann Lecun, Leon Bottou, Yoshua Bengio, and Patrick Haffner. 2021. Gradient-based learning applied to document recognition. In *Proceedings of the IEEE* 1998, 86(11):2278–2324.
- [23] Klas Leino and Matt Fredrikson. 2020. Stolen Memories: Leveraging Model Memorization for Calibrated White-Box Membership Inference. In *Proceedings of USENIX Security Symposium*, USENIX Security. 1605–1622.
- [24] Shan Li, Weihong Deng, and JunPing Du. 2017. Reliable Crowdsourcing and Deep Locality-Preserving Learning for Expression Recognition in the Wild. In *Proceedings of IEEE Conference on Computer Vision and Pattern Recognition CVPR 2017*. IEEE, 2584–2593.
- [25] Tian Li, Anit Kumar Sahu, Ameet Talwalkar, and Virginia Smith. 2020. Federated learning: Challenges, methods, and future directions. *IEEE Signal Processing Magazine* 37, 3 (2020), 50–60.
- [26] Xiang Li, Kaixuan Huang, Wenhao Yang, Shusen Wang, and Zhihua Zhang. 2020. On the convergence of fedavg on non-iid data. In *Proceedings of International Conference on Learning Representations*, ICLR.
- [27] Xiang Ling, Shouling Ji, Jiaxu Zou, Jiannan Wang, Chunming Wu, Bo Li, and Ting Wang. 2019. DEEPSEC: A Uniform Platform for Security Analysis of Deep Learning Model. In *Proceedings of IEEE Symposium on Security and Privacy*, SP. 673–690.
- [28] Peter Mayer, Yixin Zou, Florian Schaub, and Adam J. Aviv. 2021. "Now I'm a bit angry: " Individuals' Awareness, Perception, and Responses to Data Breaches that Affected Them. In *Proceedings of USENIX Security Symposium*, USENIX Security. 393–410.
- [29] Brendan McMahan, Eider Moore, Daniel Ramage, Seth Hampson, and Blaise Agüera y Arcas. 2017. Communication-Efficient Learning of Deep Networks from Decentralized Data. In *Proceedings of International Conference on Artificial Intelligence and Statistics*, AISTATS, Vol. 54. 1273–1282.
- [30] Luca Melis, Congzheng Song, Emiliano De Cristofaro, and Vitaly Shmatikov. 2019. Exploiting Unintended Feature Leakage in Collaborative Learning. In *Proceedings of IEEE Symposium on Security and Privacy*, SP. 691–706.
- [31] Viraaj Mothukuri, Reza M. Parizi, Seyedamin Pouriyeh, Yan Huang, Ali Dehghantanha, and Gautam Srivastava. 2021. A survey on security and privacy of federated learning. *Future Generation Computer Systems* 115 (2021), 619–640.
- [32] Milad Nasr, Reza Shokri, and Amir Houmansadr. 2019. Comprehensive Privacy Analysis of Deep Learning: Passive and Active White-box Inference Attacks against Centralized and Federated Learning. In *Proceedings of IEEE Symposium on Security and Privacy*, SP. 739–753.
- [33] Nicolas Papernot, Martin Abadi, Úlfar Erlingsson, Ian J. Goodfellow, and Kunal Talwar. 2017. Semi-supervised Knowledge Transfer for Deep Learning from Private Training Data. In *Proceedings of International Conference on Learning Representations*, ICLR 2017.
- [34] Mathias P. M. Parisot, Balazs Pejo, and Dayana Spagnuelo. 2021. Property Inference Attacks on Convolutional Neural Networks: Influence and Implications of Target Model's Complexity. *arXiv preprint arXiv:2104.13061* (2021).
- [35] European Parliament and the Council of the European Union. 2020. General Data Protection Regulation. <https://eur-lex.europa.eu/legal-content/EN/TXT/>

HTML/?uri=CELEX:32016R0679.

[36] Apostolos Pyrgelis, Carmela Troncoso, and Emiliano De Cristofaro. 2018. Knock Knock, Who’s There? Membership Inference on Aggregate Location Data. In *Proceedings of Network and Distributed System Security Symposium, NDSS*.

[37] Jiangcheng Qin, Baisong Liu, and Jiangbo Qian. 2021. A Novel Privacy-Preserved Recommender System Framework Based On Federated Learning. In *Proceedings of International Conference on Software Engineering and Information Management, ICSIM*. 82–88.

[38] Ahmed Salem, Yang Zhang, Mathias Humbert, Pascal Berrang, Mario Fritz, and Michael Backes. 2019. ML-Leaks: Model and Data Independent Membership Inference Attacks and Defenses on Machine Learning Models. In *Proceedings of Network and Distributed System Security Symposium, NDSS*.

[39] Reza Shokri, Marco Stronati, Congzheng Song, and Vitaly Shmatikov. 2017. Membership Inference Attacks Against Machine Learning Models. In *Proceedings of IEEE Symposium on Security and Privacy, SP*. 3–18.

[40] Apoorva Singh, Tammay Sen, Sriparna Saha, and Mohammed Hasanuzzaman. 2021. Federated Multi-task Learning for Complaint Identification from Social Media Data. In *Proceedings of ACM Conference on Hypertext and Social Media, HT*. 201–210.

[41] Nitish Srivastava, Geoffrey E. Hinton, Alex Krizhevsky, Ilya Sutskever, and Ruslan Salakhutdinov. 2014. Dropout: A Simple Way to Prevent Neural Networks from Overfitting. *Journal of Machine Learning Research* 15, 1 (2014), 1929–1958.

[42] United States. 2020. California Privacy Rights Act. <https://www.cookiebot.com/en/cpra/>. Accessed Feb 05, 2021.

[43] Nguyen H. Tran, Wei Bao, Albert Zomaya, Minh N. H. Nguyen, and Choong Seon Hong. 2019. Federated Learning over Wireless Networks: Optimization Model Design and Analysis. In *Proceedings of IEEE INFOCOM 2019 - IEEE Conference on Computer Communications*. 1387–1395.

[44] Michael Carl Tschantz, Shayak Sen, and Anupam Datta. 2020. SoK: Differential Privacy as a Causal Property. In *Proceedings of IEEE Symposium on Security and Privacy, SP*. 354–371.

[45] Yuxin Wang, Zeyu Ding, Daniel Kifer, and Danfeng Zhang. 2020. CheckDP: An Automated and Integrated Approach for Proving Differential Privacy or Finding Precise Counterexamples. In *Proceedings of ACM SIGSAC Conference on Computer and Communications Security, CCS*. 919–938.

[46] Yuxin Wang, Zeyu Ding, Yingtai Xiao, Daniel Kifer, and Danfeng Zhang. 2021. DPGen: Automated Program Synthesis for Differential Privacy. In *Proceedings of ACM SIGSAC Conference on Computer and Communications Security, CCS*. 393–411.

[47] Zhibo Wang, Mengkai Song, Zhifei Zhang, Yang Song, Qian Wang, and Hairong Qi. 2019. Beyond Inferring Class Representatives: User-Level Privacy Leakage From Federated Learning. In *Proceedings of IEEE Conference on Computer Communications, INFOCOM*. 2512–2520.

[48] Nan Wu, Farhad Farokhi, David B. Smith, and Mohamed Ali Kaafer. 2020. The Value of Collaboration in Convex Machine Learning with Differential Privacy. In *Proceedings of IEEE Symposium on Security and Privacy, SP*. 304–317.

[49] Guowen Xu, Hongwei Li, Hao Ren, Kan Yang, and Robert H. Deng. 2019. Data Security Issues in Deep Learning: Attacks, Countermeasures, and Opportunities. *IEEE Communications Magazine* 57, 11 (2019), 116–122.

[50] Carl Yang and Kevin Chang. 2019. Relationship Profiling over Social Networks: Reverse Smoothness from Similarity to Closeness. In *Proceedings of SIAM International Conference on Data Mining, SDM*. 342–350.

[51] Liu Yang, Ben Tan, Vincent W Zheng, Kai Chen, and Qiang Yang. 2020. Federated recommendation systems. In *Federated Learning*. Springer, 225–239.

[52] Qiang Yang, Yang Liu, Tianjian Chen, and Yongxin Tong. 2019. Federated machine learning: Concept and applications. *ACM Transactions on Intelligent Systems and Technology TIST* 10, 2 (2019), 1–19.

[53] Lei Yu, Ling Liu, Calton Pu, Mehmet Emre Gursoy, and Stacey Truex. 2019. Differentially Private Model Publishing for Deep Learning. In *Proceedings of IEEE Symposium on Security and Privacy, SP*. 332–349.

[54] Oualid Zari, Chuan Xu, and Giovanni Neglia. 2021. Efficient passive membership inference attack in federated learning. *arXiv preprint arXiv:2111.00430* (2021).

[55] Syed Zawad, Ahsan Ali, Pin-Yu Chen, Ali Anwar, Yi Zhou, Nathalie Baracaldo, Yuan Tian, and Feng Yan. 2021. Curse or Redemption? How Data Heterogeneity Affects the Robustness of Federated Learning. In *Proceedings of AAAI Conference on Artificial Intelligence, AAAI 2021*. 10807–10814.

[56] Chaoyun Zhang, Paul Patras, and Hamed Haddadi. 2019. Deep Learning in Mobile and Wireless Networking: A Survey. *IEEE Communications Surveys Tutorials* 21, 3 (2019), 2224–2287.

[57] Yue Zhao, Meng Li, Liangzhen Lai, Naveen Suda, Damon Civin, and Vikas Chandra. 2018. Federated learning with non-iid data. *arXiv preprint arXiv:1806.00582* (2018).

[58] Chunyi Zhou, Anmin Fu, Shui Yu, Wei Yang, Huaqun Wang, and Yuqing Zhang. 2020. Privacy-Preserving Federated Learning in Fog Computing. *IEEE Internet of Things Journal, IOTJ*, 7, 11 (2020), 10782–10793.

[59] Chaoshun Zuo, Zhiqiang Lin, and Yinqian Zhang. 2019. Why Does Your Data Leak? Uncovering the Data Leakage in Cloud from Mobile Apps. In *Proceedings of IEEE Symposium on Security and Privacy, SP*. 1296–1310.